

Single image super resolution using Lifting-Based Directionlets

DR REJI A P

NSS College,Rajakumari
Kulapparachal P.O., Rajakumari
Kerala 685619
rejishreyas@gmail.com

Abstract. The single image super-resolution is the process of recovering missing high-resolution details so as to reconstruct its high resolution image(HR) from a single low resolution image (LR). Correspondences between low and high resolution image patches are learned , and applied to the test low-resolution image to recover its most likely high-resolution version. This paper proposes, a fast learning based single image super resolution method which can be used for real time applications using multiple direction wavelet transform, called Directionlets. Conventional directionlet transform is computationally very intensive, so a lifting based implementation is used here for super resolving both grey and colour images. Here two methods, directional variance method and skewed wavelet transform are used in implementing directionlet transform. From the results it is clear that directional variance method is faster than skewed wavelet method. Results using different wavelets like db4 ,bior3.3 etc are compared here. The simulation results showed that the proposed approach is faster and needs less memory compared to conventional directionlet based single image super resolution.

Keywords: Directionlet, anisotropic, super resolution,lifting.

(Received October 5th, 2021 / Accepted December 1st, 2021)

1 Introduction

Digital image processing applications like surveillance, satellite imaging, forensic science, target identification, diagnostics, need high resolution images to obtain good result. The high resolution images not only give the user a pleasing appearance but also offer additional data that is important in many applications. The image acquisition environment condition, resolution of sensors, optical technology used are some of the factors that affect the quality of digital image and usually the captured image will be a low resolution image(LR). For example getting high quality images in applications like satellite imaging is difficult since there are many factors like weather, height which cannot be controlled. High resolution images mainly depend on manufacturing technology of sensor that tries to increase the number of pixels per unit area by reducing the pixel size. But there is limitation to this pixel size reduction due to

shot noise in the sensor itself and high precision optics sensors are too expensive to use for commercial applications. Therefore, some image processing techniques are required to construct a HR image from one or more available low resolution (LR) images. LR images can be considered as under-sampled and blurred versions of the original scene. Super resolution problem is an inverse problem that refers to the process of reconstructing a HR image than what is afforded by the physical sensor through post processing, making use of one or more LR observations [1]. This techniques include up sampling the image, thereby increasing the maximum spatial frequency and removing degradations that arise during the image capture namely aliasing and blurring.

Standard interpolation techniques like cubic interpolation, spline interpolation methods consider only LR image information. That is,they only increase the pixel count without adding the extra details and the resulting image is often blurry and contains artefacts. These

techniques perform well in smoother regions of the images and tend to blur edges and other sharp details in the images. In this article a new learning based single image super resolution method using directionlet transform based on lifting scheme is presented for both grey and colour images. The concept of Directional Variance is used to implement Directionlet Transform.

2 Related work

In general, there are two types of super resolution techniques: reconstruction-based and learning-based. In reconstruction based techniques, high resolution image is recovered from several low resolution observations of the input. Impressive amount of work has been reported in this field. Frequency domain approach proposed by Tsai in "Multiframe image restoration and registration" [21] was the first work in super resolution. They considered the super resolution problem described above subject to the assumption that the low resolution frames have neither been corrupted by noise nor degraded by a blurring phenomenon. In 1990 Irani et al, proposed a method in the paper [14] which was similar to back-projection used in tomography. In tomography, images are reconstructed from their projections in many directions. It is shown by Bose et al in their paper [?] how the total least squares recursive algorithm for the real data FIR (finite impulse response) adaptive filtering problem can be applied to reconstruct a high-resolution filtered image from undersampled, noisy multiframe, when the interframe displacements are not accurately known. Michael Elad et al in 1997, proposed a unified methodology in the paper [6] toward the more complicated problem of super resolution restoration using the tools maximum likelihood (ML) estimator, the maximum a posteriori probability (MAP) estimator, and the set theoretic approach using projection onto convex sets (POCS). The same authors presented a new method in the paper "Super-resolution restoration of an image sequence: Adaptive filtering approach" [12] based on adaptive filtering theory for super resolution restoration of continuous image sequences. Nguyen et al [15] proposed efficient block circulant pre conditioners for solving the regularized super resolution problem. In paper "An efficient wavelet-based algorithm for image super-resolution" [13] the same author presents a new and efficient wavelet-based algorithm for image super-resolution. Elad et al [20] proposed a fast and robust hybrid method of super-resolution and demosaicing, based on a maximum a posteriori (MAP) estimation technique by minimizing a multi-term cost function. In the paper [?] Bose et al investigate the effect of the threshold level on reconstructed image quality in second-generation

wavelet super-resolution. The choice of optimal threshold involves a tradeoff between noise filtering and blurring introduced by thresholding.

In learning-based super resolution algorithms, a training set of available HR images are used to obtain the HR image of an image captured using a LR camera. In the training set, images are stored as patches or coefficients of feature representations like wavelet transform, DCT, etc. Unlike the reconstruction-based method which requires multiple LR input images, here only one input image (single frame image super resolution) is required. Single frame image super resolution can be used in applications where database of HR images are available. These methods are classified under the motion free super resolution scheme. In the first part of the paper [4], authors derive a sequence of analytical results which show that the reconstruction constraints provide less and less useful information as the magnification factor increases. The paper [2] describes a new framework for processing images by example, called image analogies. In paper [24], Freeman et al propose an example based super resolution method in which he had developed a Bayesian propagation algorithm using Markov Network. Pickup et al presented a domain-specific image prior in the form of a p.d.f. based upon sampled images in the paper [16]. The paper "Learning based super-resolution imaging: Use of zoom as a cue" [9] propose a technique for super-resolution imaging of a scene from observations at different camera zooms. Given a sequence of images with different zoom factors of a static scene, they obtain a picture of the entire scene at a resolution corresponding to the most zoomed observation. In this paper [1], Jiji et al propose a single frame, learning-based super-resolution restoration technique by using the wavelet domain to define a constraint on the solution. In paper [5] Jiji et al propose a learning-based, single-image super-resolution reconstruction technique using the contourlet transform, which is capable of capturing the smoothness along contours making use of directional decompositions. In the paper [11], Pickup et al attempt to shed some light on this problem when the SR algorithms are designed for general natural images (GNIs). In the paper [8] Isabelle presents comparisons of two learning-based super-resolution algorithms as well as standard interpolation methods. In the paper "Single frame image super-resolution: should we process locally or globally?" [5] authors study the usefulness of different local and global, learning-based, single-frame image super-resolution reconstruction techniques in handling three specific tasks, namely, de-blurring, de-noising and alias removal. In the paper [18] Freeman et al introduce a

method to remove the effects of camera shake from seriously blurred images. The paper[19] "Learning the kernel matrix for super resolution" proposes the application of learned kernels in support vector regression to super resolution in the discrete cosine transform (DCT) domain. The paper [3], Ayan et al present a learning-based method to super-resolve face images using a kernel principal component analysis-based prior model. In the paper titled "Psf recovery from examples for blind super-resolution"[7], the authors propose a new learning based approach for super-resolving an image captured at low spatial resolution. Authors present a new fast method in [10]. In this paper[26] authors propose dense feature fusion (DFF) for image super-resolution (SR). In the paper [17] authors proposed a super resolution method based on conventional directionlet transform. In the new proposed method conventional directionlet transform is modified using lifting based directionlet transform .Concept of directional variance is also used to implement Directionlet transform.

This paper is organised as follows. In Section 3, the concepts of Directional transform are presented. This section explains concept of lattice based transform and directional variance in the implementation of Directionlet transform . The theory of lifting based directionlet transform is explained in Section 4. Experimental results with commonly used grey-scale and colour test images and the comparison with previous works are presented in Section 5. Finally, conclusions are given in Section 6.

3 Directionlet transform

The directionlet transform (DT) is skewed anisotropic transform and it is an efficient tool for representing images which contains multiple direction oriented and elongated edges. In DT, transforms are applied along random directions (skewed) and number of transforms are not equal (anisotropic), that is, n_1 in one direction and n_2 in other direction, where n_1 is not necessarily equal to n_2 . This process is continued in the lower sub-band, as in the standard wavelet transform to obtain multi level transform. Anisotropic transform is represented as AWT(n_1, n_2). Figure 1 shows filtering scheme of dT with when $n_1 = 2, n_2 = 1$, AWT(2,1). The next level decomposition is obtained by repeating the process in the sub band AL.

%beginfigure

Directionlet transform is obtained by applying transform in two random directions, not necessarily along horizontal and vertical directions. A problem called directional interaction is occurred if the transforms are taken in two random digital lines. The con-

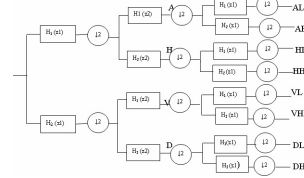


Figure 1: Filtering scheme for the AWT (2,1), where one step of iteration is shown

cept of digital lines is not enough to provide a systematic rule for sub sampling, so the concept of integer lattices is proposed by Velisavljevic et al [22] to overcome this problem.

3.1 Lattice based Transform

An integer lattice A can be represented as a collection of points obtained by taking linear combinations of two linearly independent digital lines with slopes m_1 and m_2 . The lattice A can be represented using a generator matrix X given by;

$$X = \begin{bmatrix} a & b \\ c & d \end{bmatrix} \quad (1)$$

where a, b, c and d are integers. The slopes of digital lines $m_1 = b/a$ and $m_2 = d/c$ which constitute the lattice are obtained from these integers. Figure?? shows an example of integer lattice with generator matrix M_1

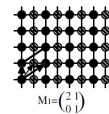


Figure 2: Lattice with generator matrix M_1

$$M_1 = \begin{bmatrix} 2 & 1 \\ 0 & 1 \end{bmatrix} \quad (2)$$

According to lattice theory concept [?], integer lattice A can be partitioned into $\det(M_1)$ cosets. Each coset is identified by shift vectors s_k , where $k = 0, 1, \dots, \det M_1 - 1$. The shift vector shows how much the coset is shifted from the origin. Each coset is a shifted version of lattice A . Intersection of each coset and digital line is called co-line. The lattice A with the corresponding generator matrix M_1 , partitions each digital line into co-lines of cosets . The lattice A with generator matrix M_1 shown in Figure is divided into 2 cosets ($\det X_1 = 2$). The black dots form the first coset

with shift vector $s_0 = (0, 0)$, shaded dots form the second coset with shift vector $s_1 = (1, 1)$.

Directionlet transform is obtained by applying 1-D wavelet transform and subsampling along co-lines with the first slope m_1 for all cosets of the lattice. The process is repeated along colines with the second slope m_2 . The sub sampled corresponding lattice is clearly a sublattice of the initial one containing a quarter of the samples[23]. For constructing the Directionlet transform, the image is partitioned into integer lattices, where the 1D filtering is performed along co-lines across the lattice.

3.2 Directional variance

Directional information locally varies in an image. Directionlet transform is obtained by applying transform along colines in selected pair of directions, for that appropriate directions for the image segment must be selected. Here the concept of directional variance is introduced to select the appropriate directions. In this paper, the input image is first divided into spatial segments of smaller size. A digital line $L(m, r)$ is defined as the set of pixels (i, j) where m is any rational slope. The directional variance for a given image segment X , along the lines with rational slope m , is defined as

$$dirvariance = \sum_{i=1}^n X \quad (3)$$

$$v = \sum_{i=1}^n \sum_{j=1}^{k_i} ((X_j - X_L(r, i))^2) \quad (4)$$

where $X_L(r, i)$ is the mean of the digital line with slope m and X_j is the pixel in the same line. N is the total number of pixels in the segment X , n is the total number of lines, and k_i is the number pixels in line.

4 Lifting scheme based directionlet transform

4.1 Lifting scheme for wavelet transform

Lifting scheme proposed by Wim Sweldons is an alternate method to construct the second generation wavelets [25].

In lifting scheme, 1-D transform is implemented in three steps: split, predict and update.

1. Split : The signal is split into two disjoint sets of even indexed samples and odd indexed samples and each set contains half samples of original signal. The process of splitting the original signal is

called the lazy wavelet transform.

$$s_{j,2l} = s_{2l} \quad (5)$$

$$s_{j,2l+1} = s_{2l+1} \quad (6)$$

2. Predict(Dual lifting): The even and odd subsets are interspersed. If the signal has a local correlation structure, the even and odd subsets will be highly correlated with each other. It means given one of the two sets, it should be possible to predict the other one with reasonable accuracy. This step is also called dual lifting. Here the odd indexed samples $s_{j,2l+1}$ are predicted using the neighboring even indexed samples $s_{j,2l}$ and the prediction error. The difference between the odd sample and its prediction replaces the original odd sample values, thus providing in-place calculations and are called detail (wavelet) coefficients.

$$d_{j-1,l} = s_{j,2l+1}(n) - P(s_{j,2l}) \quad (7)$$

3. Update : In the second lifting step, known as primal lifting (U), the even samples are replaced with smoothed values. The U operator is designed to maintain the correct running average of the original sequence, in order to avoid aliasing.

$$s_{j-1,l} = s_{j,2l} + U(d_{j-1,l}) \quad (8)$$

4. Normalize: The outputs are weighted by k_e and k_o . These values normalize the energy of the underlying scaling and wavelet functions, respectively.

Iteration of these steps creates the complete set of DWT scaling and wavelet coefficients s and d . The lifting steps are invertible, though P and U are nonlinear, space-varying, or non-invertible. The inverse lifting steps include following four steps : (i) Undo Normalize(ii) Undo Update(iii) Undo Predict (iv) Merge.

4.2 Wavelet transform in polyphase form

In filter bank representation of DWT, the forward transform uses two analysis filters \tilde{h} and \tilde{g} followed by subsampling, while the inverse transform involves up-sampling and then uses two synthesis filters h and g . For perfect reconstruction, the conditions are given by equation 9.

$$h(z)\tilde{h}(z^{-1}) + g(z)\tilde{g}(z^{-1}) = 2$$

$$h(z)\tilde{h}(-z^{-1}) + g(z)\tilde{g}(-z^{-1}) = 0 \quad (9)$$

Based on Polyphase representation a filter $h(z)$ can be represented by

$$h(z) = \sum_{k=-\infty}^{\infty} h(k)z^{-k} \quad (10)$$

Using polyphase representation, discrete time filter can be represented by the equation 11, where h_e and h_o are even and odd coefficients [?].

$$h(z) = h_e(z^2) + z^{-1}h_o(z^2) \quad (11)$$

$$h_e[z] = \sum h_{2k}z^{-k} \quad (12)$$

$$h_o[z] = \sum h_{2k+1}z^{-k} \quad (13)$$

The polyphase decomposition can be used to implement filter bank in efficient manner. The wavelet transform is represented by schematically in Figure 3. $P(z)$ is called polyphase matrix for synthesis and is represented by;

$$P(z) = \begin{bmatrix} h_e(z) & g_e(z) \\ h_o(z) & g_o(z) \end{bmatrix} \quad (14)$$

%beginfigure

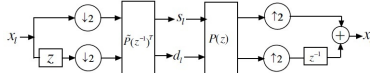


Figure 3: Polyphase representation of wavelet transform

In polyphase representation sequence is divided into odd or even and then apply the poly phase matrix. In inverse transform, the polyphase matrix is followed by merging odd and even samples. The perfect reconstruction property is given by;

$$P(z)\tilde{P}(z^{-1})^t = I \quad (15)$$

where $\tilde{P}(z)$ is called polyphase matrix for analysis bank.

4.3 Polyphase representation of lifting method

The polyphase representation is an effective way of representing lifting method. As already explained, lifting consists of three steps: split, predict, and update. The odd/even split is another form of polyphase domain. For a given complementary filter pair (h, g), the polyphase matrix in equation 14 can be factored using Laurent polynomials $s_i(z)$, $t_i(z)$ and non zero constant

K . Euclidian algorithm can be used to factor poly phase matrix. The equation 16 show the factorisation of $P(z)$.

$$P(z) = \prod_1^m \begin{bmatrix} 1 & s_i(z) \\ 0 & 1 \end{bmatrix} * \begin{bmatrix} 1 & 0 \\ t_i(z) & 1 \end{bmatrix} * \begin{bmatrix} K & 0 \\ 1 & 1/K \end{bmatrix} \quad (16)$$

The dual polyphase matrix is given by

$$\tilde{P} = \prod_1^m \begin{bmatrix} 1 & 0 \\ -s_i(z^{-1}) & 1 \end{bmatrix} * \begin{bmatrix} 1 & 0 \\ -t_i(z^{-1}) & 1 \end{bmatrix} \begin{bmatrix} 1/K & 0 \\ 1 & K \end{bmatrix} \quad (17)$$

The polynomial $s_i(z)$ represents primary lifting steps and $t_i(z)$ represents dual lifting steps.

4.4 Lifting scheme for directionlet transform

Since Directionlet uses lattice based filtering and sub-sampling, the lifting framework can be used to represent the lattice based transform. To implement directionlet transform, lifting based wavelet transform is applied along selected pair of directions. The lifting steps are :

1. Split step : Split the pixels of lattice A located along the transform direction d_1 , $x(n)$ into two disjoint subsets: the odd and even polyphase samples $x_o(n)$ and $x_e(n)$. Here $x_e(n) = x(2n)$ and $x_o(n) = x(2n + 1)$.
2. Prediction step: The wavelet coefficients or detail signal $d[n]$ is generated as error in predicting $x_o(n)$ from $x_e(n)$ using prediction operator P , by keeping even samples changeless. The difference between the prediction value of $x_o(n)$ and the real value of $x_o(n)$ is defined as the high-frequency component or detail signal.

$$d(n) = x_o(n) - P(x_e(n)) \quad (18)$$

3. Update step: This detail coefficients are used to update even samples $x_e(n)$, to obtain the approximate signal which creates the low-frequency component. $x_e(n)$ and $d(n)$ are combined to obtain scaling coefficients $c(n)$ which is a coarse approximation to the original signal $x(n)$. This is done by applying an update operator U to the wavelet coefficients $d(n)$ and adding the result to $x_e(n)$:

$$c(n) = x_e(n) + U(d(n)) \quad (19)$$

By performing the above process along co-lines in all cosets in both directions, the multi resolution lifting directionlet decomposition is obtained.

5 Single Image Super Resolution using directionlets based on lifting scheme

5.1 Low resolution model

Single frame super-resolution algorithms attempt to estimate high resolution image from single low resolution observation. The first step to comprehensively analyze the super resolution image problem is to formulate an observation model that relates the original image (HR) to the observed LR image. Usually super resolution problem can be modeled using equation 20, given by;

$$Y = DBZ + n \quad (20)$$

The low resolution pixel intensity is the average of high resolution intensities over a neighborhood of 4 pixels. Y represents the lexicographically ordered vector of size $M^2 \times 1$, which is formed from the observed low resolution image of size $M \times M$. Z is the lexicographically ordered vector of the high resolution image to be super resolved. Here n is the independent and identically distributed (i.i.d.) noise vector with zero mean and variance σ . It has same size as Y . Here the problem is to estimate Z , the HR image, given Y , the LR image. B is blurred matrix considered as an identity matrix. Generally, the decimation matrix D , used to obtain the aliased pixel intensities from the high resolution image is given as;

$$D = \begin{bmatrix} 11..1 & & 0 \\ & 11..1 & \\ 0 & & 11..1 \end{bmatrix} \quad (21)$$

For example, with decimation factor $q = 2$ and with lexicographically ordered Z of size, say 16×1 , the D matrix of size 4×16 can be written as

$$D = \begin{bmatrix} 1100110000000000 \\ 0011001100000000 \\ 0000000011001100 \\ 0000000000110011 \end{bmatrix} \quad (22)$$

Thus equation 20 indicates that the low resolution pixel intensity is obtained by averaging the intensities of q^2 pixels corresponding to the same scene in the high resolution image and adding noise.

5.2 Single image super resolution method using critically sampled directionlets

Critically sampled directionlet transform involves filtering followed by sub sampling. Critically sampled directionlets are used to extract directional features present in images.

5.2.1 Training set generation

To generate a training set, a collection of high resolution images and their low resolution (LR) images are used. LR images are formed by averaging the intensities of non overlapping block of size 2×2 pixels from HR image, (where 2 is the decimation factor) using the equation 20. In the case of images, the directional information varies over space. Thus, directionality can be considered as a local feature, defined in a small neighborhood. Therefore, to extract directional variations of an image it has to be analysed locally. For this, the HR and LR images are subdivided into patches of size 8×8 and 4×4 , respectively in raster scan order. To avoid a blocking effect in the transform caused by the small patches, overlapping blocks are used. ie; extra pixels from neighboring patches are added on four sides to avoid errors in borders.

The super resolution algorithm also operates under the assumption that the predictive relationship between low and high resolution images is independent of local image contrast. Because of this, patch pairs of high and low resolution images are contrast normalized by the energy of the low-resolution patch. Energy of low resolution patch is obtained by the equation,

$$energy = 0.01 + \Sigma \sqrt{y_k^2} \quad (23)$$

where k is the value of the pixel number in the LR patch. The constant 0.01 is added to prevent division by zero.

5.3 Determination of best pair of direction for a patch

Two methods are used to select the best pair of directions

5.3.1 Directional variance method

To apply the directionlet transform, optimum pair of direction must be selected. The directional variance is computed along the rational directions $(i, j) = (1, 0), (1, 1), (0, 1), (-1, 1)$, which corresponds to $0^\circ, 45^\circ, 90^\circ$ and -45° . The directions corresponding to the two minimum directional variances are identified and these are selected as the pair of directions for computing the directionlet transform. The assigned best pair of transform directions of each patch form a directional map of that LR image and its corresponding HR image.

5.3.2 Skewed wavelet transform method

Wavelet transform filtering and subsampling are done along different pair of directions $(0^\circ, 45^\circ), (0^\circ, -45^\circ), (90^\circ, 45^\circ), (90^\circ, -45^\circ), (0^\circ, 90^\circ)$ and selected the pair

of directions with minimum energy as best pair of directions.

It is seen that the directional variance method is faster than wavelet method and produces comparable result as shown in table 1.

Table 1: Time taken to super resolve images with skewed wavelet method and directional variance method

| Input images | | time in seconds | |
|--------------|---------|-----------------|------------|
| name | size | method1 | new method |
| image 1 | 256x256 | 365 | 270 |
| image2 | 256x256 | 358 | 218 |

5.4 Implementation

5.4.1 Implementation of db4 wavelet using lifting method

Table 2: Wavelet coefficients of db4

| low pass filter | | high pass filter | |
|-----------------|---------|------------------|---------|
| h_0 | -0.0106 | g_7 | -0.2304 |
| h_1 | 0.0329 | g_6 | 0.7148 |
| h_2 | 0.0308 | g_5 | 0.6309 |
| h_3 | -0.1870 | g_4 | -0.0280 |
| h_4 | -0.0280 | g_3 | -0.1870 |
| h_5 | 0.6309 | g_2 | 0.0308 |
| h_6 | 0.7148 | g_1 | 0.0329 |
| h_7 | 0.2304 | g_0 | -0.0106 |

Wavelet coefficients for db4 are shown in table 2. The lifting coefficients are different for different wavelets. These coefficients are obtained from wavelet coefficients. Table 3 shows the db4 coefficients used in the lifting scheme.

Table 3: Coefficients in lifting steps

| | |
|-------------|-------------------|
| k_1 | 1.362166720130752 |
| λ_0 | -1 |
| λ_1 | 0.469083478901698 |
| λ_2 | 0.14003923772683 |
| λ_3 | 0.024791238156143 |
| η | 2.131816712755221 |
| γ^1 | 0.117648086798478 |
| γ | 0.018808352726244 |
| β^1 | 0.300142258748545 |
| β | 1.117123605160594 |
| α | 0.322275887997141 |

Euclid algorithm can be used to find DWT with a finite number of lifting steps starting from polyphase

transform. db4 wavelet transform can be expressed into lifting steps as follows,

1. db4 wavelet is an orthogonal base. Inverse transform uses two synthesis filters h and g. Under the perfect reconstruction condition,

$$\begin{aligned}
 h(z) &= h(0) + h_1 z^{-1} + h_2 z^{-2} + h_3 z^{-3} \\
 &+ h_4 z^{-4} + h_5 z^{-5} + h_6 z^{-7} + h_7 z^{-8} \\
 g(z) &= h_7 z^6 + h_6 z^5 + h_5 z^4 + h_4 z^3 \\
 &+ h_3 z^2 + h_2 z^1 + h_1 z + h_0 z^{-1}
 \end{aligned} \quad (24)$$

Polyphase representation of synthesis filters is given by equations 25 and 26.

$$h(z) = h_e(z^2) + z^{-1} h_o z^2 \quad (25)$$

$$g(z) = g_e(z^2) + z^{-1} g_o z^2 \quad (26)$$

h_e contains the even coefficients, and h_o contains the odd coefficients.

2. Using polyphase representation of db4 synthesis filters h and g, synthesis polyphase matrix P(z) is obtained. Synthesis polyphase matrix is given by equation 27

$$P(z) = \begin{bmatrix} h_e(z) & g_e(z) \\ h_o(z) & g_o(z) \end{bmatrix} \quad (27)$$

$$h_e(z) = h_0 + h_2 z^{-1} + h_4 z^{-2} + h_6 z^{-3} \quad (28)$$

$$h_o(z) = h_1 + h_3 z^{-1} + h_5 z^{-2} + h_7 z^{-3} \quad (29)$$

$$g_e(z) = h_7 z^3 + h_5 z^2 + h_3 z + h_1 \quad (30)$$

$$g_o(z) = -h_6 z^3 - h_4 z^2 - h_2 z^1 - h_0 \quad (31)$$

Polyphase representation of wavelet transforms is shown in Figure 3.

3. Using Euclidean algorithm for Laurent polynomial, synthesis polyphase matrix P(z) can be factored into lifting steps.

$$\begin{aligned}
 P(z) &= \begin{bmatrix} 1 & 0 \\ -\alpha & 1 \end{bmatrix} * \begin{bmatrix} 1 & (\beta z^{-1} + \beta') \\ 0 & 1 \end{bmatrix} \\
 & * \begin{bmatrix} 1 & 0 \\ (\gamma z^{-1} + \gamma') & 1 \end{bmatrix} \\
 & * \begin{bmatrix} 1 & (\eta z^{-1} + \eta') \\ 0 & 1 \end{bmatrix} * \begin{bmatrix} 1 & 0 \\ 1 & 1 \end{bmatrix} \\
 & * \begin{bmatrix} 1 & -1 \\ 0 & 1 \end{bmatrix} * \begin{bmatrix} 1 & -(\lambda_3 z^3 + \lambda_2 z^2 + \lambda_1 z + \lambda_0) \\ 0 & 1 \end{bmatrix} \\
 & * \begin{bmatrix} -K^{-1} & 0 \\ 0 & K \end{bmatrix} \quad (32)
 \end{aligned}$$

The coefficients α, β etc in above equation can be obtained from Matlab 7.0 by the command function *lifftwave()*, and are listed in table 3.

4. Obtain analysis polyphase matrix $\tilde{P}(z^{-1})^T$.

$$\tilde{P}(z^{-1})^T = P(Z^{-1})^T \quad (33)$$

The analysis polyphase matrix is factored as follows

$$\begin{aligned} \tilde{P}(z^{-1})^T &= \begin{bmatrix} -k_1^{-1} & 0 \\ 0 & K_1 \end{bmatrix} \\ &* \begin{bmatrix} 1 & 0 \\ -(\lambda_3 z^{-3} + \lambda_2 z^{-2} + \lambda_1 z^{-1} + \lambda_0) & 1 \end{bmatrix} \\ &\begin{bmatrix} 1 & 0 \\ -1 & 1 \end{bmatrix} * \begin{bmatrix} 1 & 1 \\ 0 & 1 \end{bmatrix} * \begin{bmatrix} 1 & 0 \\ (\eta z + \eta') & 1 \end{bmatrix} \\ &* \begin{bmatrix} 1 & 0 \\ -(\gamma z + \gamma') & 1 \end{bmatrix} \\ &\begin{bmatrix} 1 & 0 \\ (\beta z + \beta') & 1 \end{bmatrix} * \begin{bmatrix} -K^{-1} & 0 \\ 0 & K \end{bmatrix} \quad (34) \end{aligned}$$

This corresponds to the following implementation for the forward transform:

$$s(l)^1 = x(2l + 1) + \alpha x(2l) \quad (35)$$

$$d(l)^1 = -\beta s_{l+1}^1 + \beta s_l^1 + x_{2l+1} \quad (36)$$

$$s(l)^2 = s_l^1 - \gamma d_{l+1}^1 - \gamma' d_l^1 \quad (37)$$

$$d(l)^2 = -\eta s_{l+1}^2 - \eta' s_l^2 + d_l^1 \quad (38)$$

$$s(l)^3 = s(l)^2 + d(l)^2 \quad (39)$$

$$d(l)^3 = -s(l)^3 + d(l)^2 \quad (40)$$

$$d^4 = -\lambda_3 s_{l-3}^3 - \lambda_2 s_{l-2}^3 - \lambda_1 s_{l-1}^3 \quad (41)$$

$$+s(l)^3 + d_l^3 \quad (42)$$

$$s(l) = -k_l^{-1} s(l)^3 \quad (43)$$

$$d(l) = -k_1 d(l)^4 \quad (44)$$

where s_l and d_l are smoothed values and details respectively.

5. Derive the inverse transform from the forward by running the scheme backward

5.4.2 Implementation of directionlet transform using db4 wavelet

Here the directionlet transform is implemented by applying lifting based 1-D wavelet transform along selected pair of directions. Here also lattice structure

based filtering and subsampling are used. The same set of directions used in conventional directionlet method are used here.

5.4.3 Development of training set

The training set is obtained from high resolution images downloaded from internet. One of the training set is shown in Figure4. This image is selected as training set image because it contains information in five pair of directions. It is of size 333x500 and in tiff format.



Figure 4: Training set image

5.5 Results and discussion

Experiments were performed for various types of grey images, using a training set which contained good quality images having various levels of information content. The important thing is that training set is not specific to the class of objects to be super resolved. For finding the directionlet transform db4 wavelet basis was used. The low resolution images are super resolved to double size. ie; the magnification factor is 2.

Table 4: SNR values for different images with traditional directionlet method and lifting based directionlet method

| Method | SNR in dB | | |
|----------------------|-----------|-----------|--------|
| | Barbara | Butterfly | Tiger |
| cubic spline method | 15.59 | 22.74 | 22.611 |
| directionlet method | 20.34 | 26.79 | 25.15 |
| lifting based method | 20.35 | 26.80 | 25.26 |

SNR values obtained for different standard images using cubic spline interpolation method, conventional directionlet transform and lifting scheme based are shown in table 4. The time taken for training set formation and learning process is shown in tables 5 and 6 respectively. The SNR value obtained for super resolving image1 of size 256x256 to the size of 512x512 with conventional directionlet method is 20.3445dB while with lifting scheme based method it is 20.3513dB. SNR values show that both methods give almost same SNR values. It is clear from the table 6 that time taken to super resolve an image of size 256 × 256 to the size

of 512×512 , using conventional directionlet method is 1841.033 seconds while that with lifting based directionlet it is 973.135 seconds. While the average time to convert an image of size 128×128 to an image of size 256×256 the traditional directionlet method needs 1142.806 seconds, lifting method requires only 288.523 seconds.

Table 5: Time taken to generate training set with high resolution images of different size with traditional directionlet method and lifting based directionlet method

| Input images | | Time in seconds | |
|--------------|---------|-----------------|------------|
| name | size | Old method | New method |
| image 1 | 256x256 | 625.55 | 294.18 |
| image2 | 128x128 | 71.42 | 67.21 |
| image3 | 500x233 | 1698.82 | 855.52 |

Table 6: Time taken to super resolve low resolution images of different size with traditional directionlet method and lifting based directionlet method

| Input images | | Time in seconds | |
|--------------|---------|-----------------|------------|
| name | size | Old method | New method |
| image 1 | 500x233 | 3684.76 | 2017.31 |
| image2 | 128x128 | 1142.80 | 288.52 |
| image3 | 256x256 | 1841.03 | 973.13 |

Figures 5, show results of super resolving LR images of size 128×128 to 256×256 using conventional directionlet transform and lifting based directionlet transform. Figure 5 (a) is the original image (it is shown here for comparison) (b) is the cubic spline interpolated image (c) super resolved image using lifting method based super resolution (d) super resolved image using conventional directionlet method. Cubic spline image shows artefacts in lines of scarf and it is almost removed in Figures 5 (c) and (d) and both images are of same quality. Figure 6(a) is the original image (b) is the cubic spline interpolated image (c) super resolved image using lifting method, (d) super resolved image using conventional directionlet method. From them, it is clear that both methods give almost same result. It is also obvious that using new directionlet method low resolution image of any size can be super resolved.

6 conclusion

In this article a new method for super resolving a low resolution image using learning based approach is presented. This is done using lifting based directionlet transform. Instead of the conventional filter bank implementation scheme, this article proposes a computationally less intensive method, namely lifting based



Figure 5: (a)Original image(b)cubic spline interpolated image(c)super resolved using lifting based directionlet(d)super resolved using convolution based directionlet(e),(f),(g),(h)zoomed portion of the face of (a),(b),(c),(d)respy

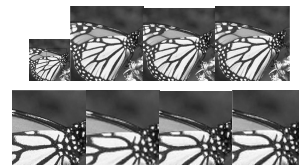


Figure 6: (a)Original image(b)cubic spline interpolated image(c)super resolved using lifting based directionlet(d)super resolved using convolution based directionlet(e),(f),(g),(h)zoomed portion of the face of (a),(b),(c),(d)respy

directionlet transform. Concept of directional variance is used to implement the directionlet transform. As a result, tremendous reduction in computation has been achieved. The method implemented using lifting based Directionlet transform and directional variance is faster than the Filter Bank scheme; especially when the filter has more taps. The capability and time saving achieved by combining directionlet transform and lifting scheme will be very useful in real time super resolution problems. db4 wavelet has been chosen for the simulation.

References

- [1] Aaron.Hertzmann, Jacobs, C., and Salesin. Single frame image super-resolution using learned wavelet coefficients. *International Journal of Imaging Systems and Technology*, 14:105–112, 2004.
- [2] Aaron.Hertzmann, C. J., N. O. B. C. and Salesin.
- [3] Ayan.Chakrabarti, R. and Rama.Chellappa. Ieee transactions on multimedia. 9:888892, 2007.
- [4] Baker.S and Kanade.T. Proceedings. ieee conference on computer vision and pattern recognition. 12:372 379, 2000.
- [5] C.V.Jiji, S. and Priyam.Chatterjee. Single frame image super-resolution: should we process locally

- or globally? *Multidimensional Systems and Signal Processing*, 18:123152, 2007.
- [6] Elad.M and Feuer.A. Restoration of a single super resolution image from several blurred, noisy, and under sampled measured image. *IEEE Transactions on Image Processing*, 6:1646–1658, 1997.
- [7] Gajjar.P.P, frame superresolution: A new learning based approach, J. S., use of igmrf prior". ICVGIP 08. Sixth Indian Conference on Computer Vision, G., and Image Processing, ., 17:636643. Icvqip 08. sixth indian conference on computer vision, graphics and image processing. 17:636643, 2008.
- [8] Isabelle.B and Frank.P.Ferrie. Comparison of super-resolution algorithms using image quality measures. *The 3rd Canadian Conference on Computer and Robot Vision*, 3:439448, 2006.
- [9] Joshi.M.V, C. and Panuganti.R. Learning based super-resolution imaging: Use of zoom as a cue. *IEEE Transactions on Systems, Man, and Cybernetics Part B*, 16:527537, 2003.
- [10] Kumar, N. and Sethi. Proceedings of the ieee conference on computer vision and pattern recognition (cvpr). 136:24722481, 2016.
- [11] Lyndsey.Pickup, S. and Andrew.Zisserman. Optimizing and learning for super-resolution. In *Chantler,M.J, Trucco, E. and Fisher, R.B (eds) Proc. British Machine Vision Conf*, 3:439448, 2006.
- [12] Michael.Elad and Arie.Feuer. Superresolution restoration of an image sequence: Adaptive filtering approach. *IEEE transactions on image processing*, 8:387–395, 1999.
- [13] Nhat.Nguyen. Ieee trans.on parallel and distributed systems. 16:3259–3252, 2000.
- [14] N.K.Bose, H. and H.M.Valenzuela. Recursive implementation of total least squares algorithm for image reconstruction from noisy, undersampled multiframe. *Proc. IEEE Conf. Acoustics, Speech and Signal Processing, Minneapolis*, 5:269–272, 1993.
- [15] Peyman.Milanfar, N. and Gene.golub. Pre conditioners for regularised image super resolution. *Proceedings IEEE International Conference on Acoustics, Speech, and Signal Processing*, 6:3259–3252, 1999.
- [16] Pickup.L.C, R. Z. A. A sample texture prior for image super-resolution advances. *I Neural Information Processing Systems*, 82:1587–1594, 2003.
- [17] Reji.A.P and Dr.Tessamma.Thomas. directionally adaptive techniques for single image superresolution). *International journal of Innovative Computing and Applications*, 3:117125, 2010.
- [18] Rob.Fergus, B. H. A. R. S. T., Singh and Freeman, W. T. Removing camera shake from a single photograph. *ACM Transactions on Graphics (TOG)*, 3:439448, 2006.
- [19] Sanjeev.K and Nguyen.T. Learning the kernel matrix for superresolution. *IEEE 8th Workshop on Multimedia Signal Processing*, 3:441446, 2006.
- [20] Sina.Farsiu, M. and Peyman.Milanfar. Multiframe demosaicing and super-resolution from under-sampled color images. *IS and T/SPIE 16th Annual Sympo on Electronic Imaging*, 16:222233, 2004.
- [21] Tsai.R.Y and Huang.T.S. Multiframe image restoration and registration. *Advances in Computer Vision and Image Processing*, 22:317–339, 1984.
- [22] Velisavljevic.V, V., Beferull-Lozano.B and P.L, D. Directionlets: anisotropic multi directional representation with separable filtering). *IEEE Transactions Image Processing*, 3:1916–1933, 2006.
- [23] Vladan.Velisavljevi, M., Baltasar.Beferull-Lozano1 and Pier.Luigi.Dragotti. Discrete multi-directional wavelet bases. *In International Conference on Image processing*, 3:10258, 2003.
- [24] William.T.Freeman, T. and Egon.C.Pasztor. Example-based superresolution. *IEEE,Image-Based Modeling and Rendering, and Lighting*, 82:56–65, 2002.
- [25] Wim.Sweldens. The lifting scheme: A new philosophy in biorthogonal wavelet constructions. *Disc. Math*, 109:1326, 1992.
- [26] Yulun Zhang1, Y. T., Y. K. B. Z. Y. F. Residual dense network for image superresolution. *Proceedings of the IEEE Conference on Computer Vision and Pattern Recognition (CVPR)*, 3:439448, 2018.